Proceedings of the 9th International Conference on Cyclotrons and their Applications
September 1981, Caen, France

THE MAGNETIC FIELD OF THE K500 CYCLOTRON AT MSU INCLUDING TRIM COILS AND EXTRACTION CHANNELS*

P. Miller, D. Johnson and H. Blosser

National Superconducting Cyclotron Laboratory, Michigan State University, East Lansing, MI 48824, USA

Abstract.-A field mapping program has been carried out in the K500 cyclotron with all magnetic components in place to obtain a data in computer files needed to find operating settings for any desired beam. The set of measurements includes the effect of pole tip shims installed after previous magnetic field measurements to compensate for holes drilled for rf and trim coil penetrations. These shims produce the desired field changes. A small hysteresis effect appears in the radial profile of the average field; it is eliminated by a simple turn-on cycle. Hysteresis effects from trim coil excitations are negligible, but the trim coil field intensity depends slightly on the central field level. Also, the trim coil field is measurably stronger than the air core calculation predicts. The first harmonic of the ν_r=1 resonance is controlled by varying the current distribution in the 3 sectors of trim coils 1 and 13. The magnetic extraction elements are passive iron focusing channels, designed in the saturated iron approximation. The first harmonic of the stray field is compensated at a radius near the extraction radius. The measurements verify in detail the accuracy of stray field calculations for the focusing bars.

1.Introduction.-The K500 magnet was dismantled in spring of 1980 to install trim coils and to make penetrations through the midplane sections of the coil and cryostat for extraction elements. The location of the magnetic channels (M_1-M_8) and the magnetic compensating bars (C_1 and C_2) are given in Fig. 1. Some iron shims were also added and removed to adjust the average field and the flutter according to calculations with previously measured field maps,[1,2] The design of these shims took note of the effect of drilling 156 holes for trim coil leads and 18 others for rf couplers, trimmers etc. These additional holes, shown in Fig. 2, were drilled in the poles while the magnet was apart. After these installations, the re-assembled magnet was field mapped again starting in January 1981. These maps are the data for predicting the main coil currents, trim coil currents and focusing bar positions needed for any beam. The mapping apparatus measured the field with an accuracy of approximately ±10 G. This figure is dominated by the estimated effect of slow unpredictable changes in the calibration constants for the flip coils which occured continuously.

2. Experiments and results.-The operating region of the cyclotron, between B_o=30 kG and B_o=49 kG (B_o= central magnetic induction) was covered with a grid of 15 points in the coordinate plane defined by the currents in the small and large main coils, called I_α and I_β respectively (see Fig. 3). The accuracy of interpolation in this size grid was verified experimentally. It was necessary to develop a standard turn-on cycle to avoid a small hysteresis effect in the radial profile ($\leq$20 G). An example of this effect is shown in Fig. 4. A short circuit developed during operation at the highest excitation (I_α/I_β=600 A/800 A) which persisted thereafter but had no measurable effect on the steady state field of the magnet, although it constrained the current rampings to be slower than usual to limit the axial forces in the coil support links. Since the short circuit made it impractical to include maximum excitation in a turn-on cycle, the chosen cycle began at field 0 (see Fig. 3) and followed the solid line until the desired sum $I_\alpha+I_\beta$ was reached. Then one adjusted I_α and I_β to desired values, keeping the sum fixed.

The trim coils were mapped at 4 main excitations near the corners of the base field grid. Hysteresis effects from main coil or trim coil excitation on the trim coil - produced field were found to be negligible. The average field from each trim coil was slightly larger than the calculated field assuming air core coils and varied a few percent with excitation, presumably due to saturation of the yoke. Figure 5 shows an example of the experimental and air-core average fields.

As a check of the iron field and to verify trim coil superposition, the field was mapped with all trim coils turned on at the calculated settings for E/A = 80 MeV/u, Q/A = .5, e.g. deuterons. When the phase and focusing behavior of the particle were calculated in the measured field the results were as expected.

The shape of the edge field (R>26.5 inches) was inferred from measurements at 5 azimuths where holes exist in the median plane so the field measuring probe could be displaced radially into the coil. The field modulation was taken into account, and the average field in the region 27 in.$\leq$R$\leq$40 in. was obtained for each of the base fields. This allows the total field to be calculated at any azimuth along the trajectory of the extracted beam out to R=40 in. to an estimated accuracy of ±50 G.

3. Discussion.-The passive magnetic channels were designed using surface current (saturated iron) calculations of the field perturbations that they produce.[3] These calculations were verified experimentally in two ways:

1) The total change in field caused by the focusing bars was displayed by subtracting a field map (point by point) measured without focusing bars in the magnet from a map taken at the same coil currents after installation of all focusing bars in their center positions. This was compared directly with the field calculated by the surface current representation of the bars (see Fig. 6).

2) The changes in the field map that occurred when one or more focusing bars were moved radially outward by 0.25 inch was compared with the changes expected from the calculation. An example of these data is the graphs in Fig. 7.

Both methods show that the calculations accurately portray the field perturbations produced by the focusing bars inside the extraction radius. The first harmonic compensation is successful at all radii out to the extraction point; the second harmonic was not compensated in the design (see Fig. 8).

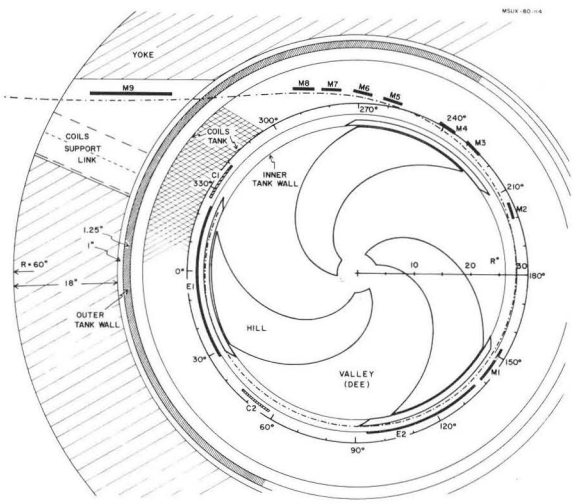

Fig. 1: Plan of the extraction system.

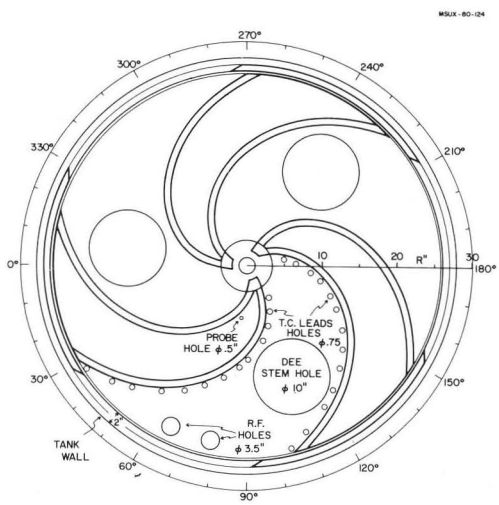

Fig. 2: Diagram of holes drilled in each sector for trim coil leads, phase slit or axial probe, rf coupler and dee tuner.

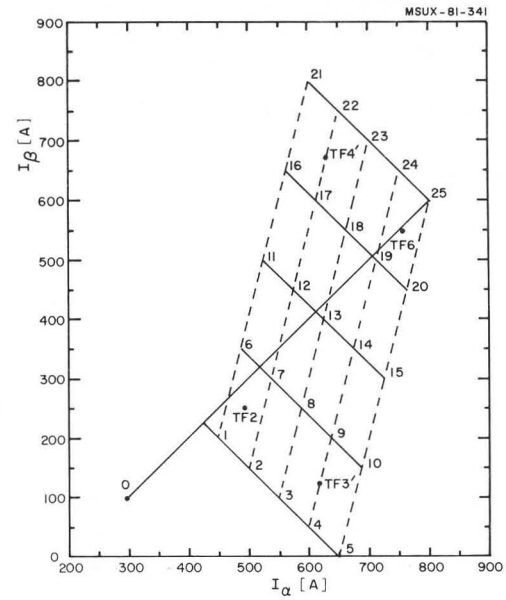

Fig. 3: Mapping grid in terms of the main coil currents I_α and I_β. The grid points at which base maps (no trim coils) were made are the center and ends of the 5 solid diagonal lines (e.g. field nos. 1, 3, 5). On these lines $I_\alpha + I_\beta$ is constant and B is approximately constant. Trim coil maps were made at TF2, TF3', TF4' and TF6. The solid lines define the path for the anti-hysteresis turn-on cycle, starting from field no. 0.

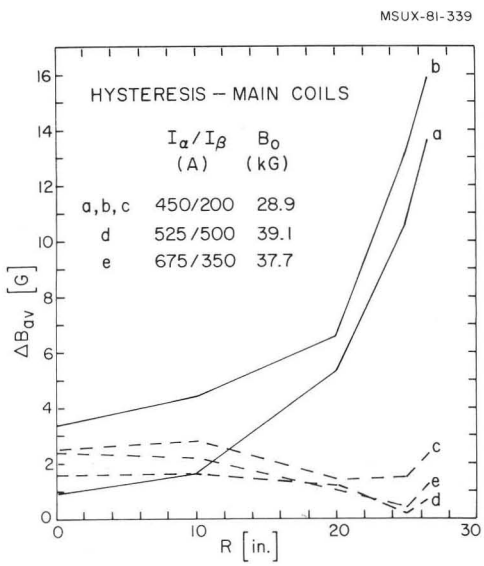

Fig. 4: Hysteresis effect on average field from main coil current variations with $I_\alpha + I_\beta$=constant. a and b have operating point approached from opposite directions; c is for same direction, which reduces hysteresis effect to the detection threshold. d and e are similar to c but for higher excitations.

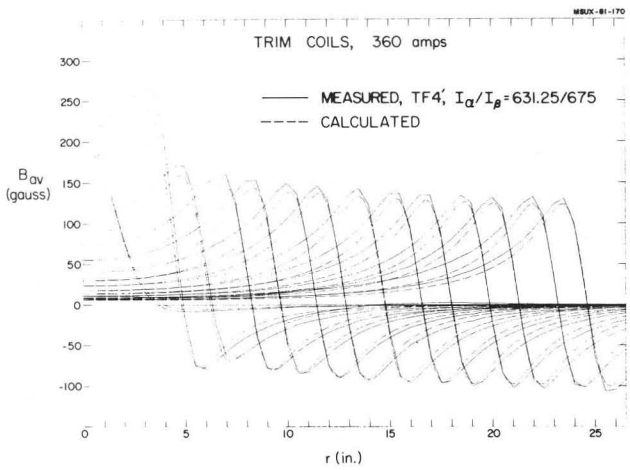

Fig. 5: Measured and calculated field profiles for trim coil O average (circular) and trim coils 1-13 (3 sectors, equal currents).

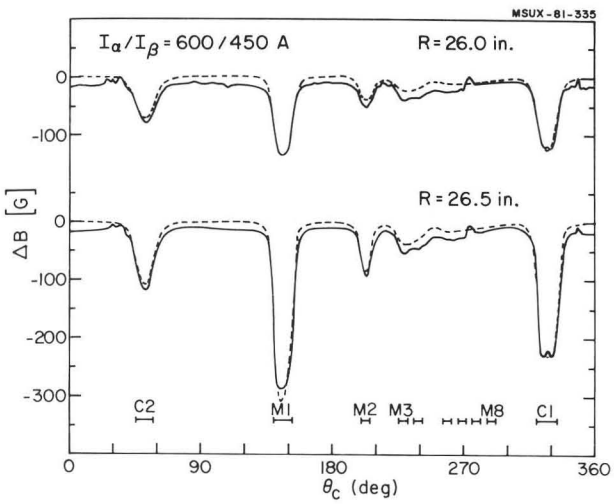

Fig. 6: Magnetic field perturbation ΔB due to installation of focusing bars M_1-M_8 and C_1 and C_2 (compensators) measured at the radius of the outer flip coil (R=26.5 inches) and the adjacent one. Solid curve was measured, at I_α/I_β=600/450 A (B_o=39.1 kG) dashed line is the calculation (surface current). The abscissa is the azimuth relative to the cyclotron reference. The zero shift of about 12 G is from a slight difference in I_α between the two maps subtracted.

4. Conclusions.-The magnetic field distribution is satisfactory for use of the cyclotron. The necessary data and procedures for obtaining settings for power supplies and focusing bar positions for any desired beam are in hand.

5. Acknowledgements.-T. Antaya, M. Distasio, H. Laumer, D. Poe and A. Zeller assisted by other staff and students ran the field mapping apparatus. B. Jeltema provided computer programming for acquiring the data.

*This material is supported by NSF Grant No. PHY. 80-17605.

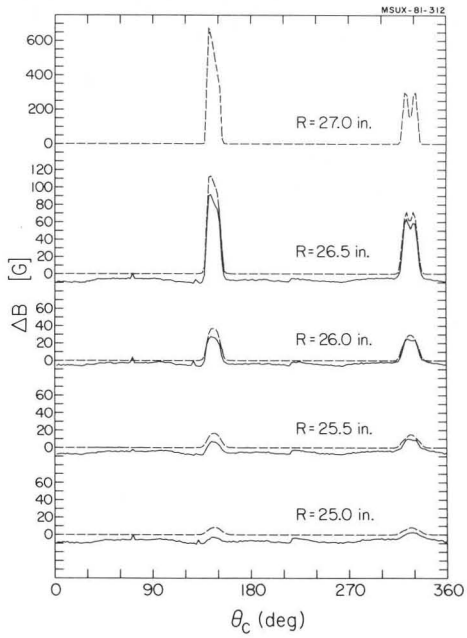

Fig. 7: Field perturbation from a radial displacement of both M_1 and C_1 by 0.25 inch.

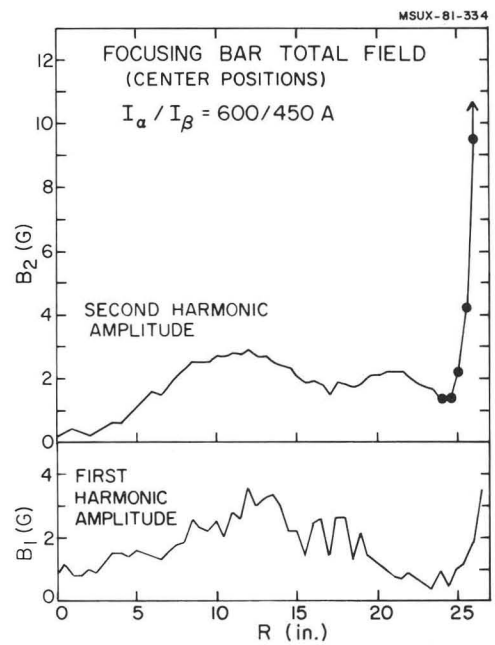

Fig. 8: First and second harmonic amplitudes of the total measured focusing bar fields (data as in Fig. 6).

References

1. G. Bellomo and F. Resmini, Nucl. Inst. Meth. 180 (1981) 305.
2. G. Bellomo et al., Nucl. Inst. Meth. 180 (1981) 285.
3. E. Fabrici et al., Nucl. Inst. Meth. 184 (1981) 301.